Nationaal Lucht- en Ruimtevaartlaboratorium
National Aerospace Laboratory NLR

NLR-TP-2001-149

Active control of rotor-stator interaction noise through vibrating vanes

J.B.H.M. Schulten

Nationaal Lucht- en Ruimtevaartlaboratorium
National Aerospace Laboratory NLR

NLR-TP-2001-149

Active control of rotor-stator interaction noise through vibrating vanes

J.B.H.M. Schulten

The contents of this report have been initially prepared for publication as AIAA paper 2001-2151 in the Proceedings of the 7th AIAA/CEAS Aeroacoustics Conference, Maastricht, The Netherlands, 28-30 May 2001.

Division: Fluid Dynamics
Issued: 2 April 2001
Classification of title: Unclassified

Contents

6 tables
22 figures

(11 pages in total)

2001-2151

ACTIVE CONTROL OF ROTOR-STATOR INTERACTION NOISE THROUGH VIBRATING VANES

Johan B.H.M. Schulten*
National Aerospace Laboratory NLR, 8300 AD Emmeloord, The Netherlands

Abstract

A theoretical study on the potential of controlled vane vibration to reduce rotor-stator interaction noise is presented. A lifting surface method was applied to compute the interaction of viscous rotor wakes with vanes in a realistic fan configuration. The lifting surface modeling was extended to include a vibration in pitch of the unswept stator vanes. Three active control parameters were used for optimization: phase and amplitude as well as the pitch axis location. The method is demonstrated for typical approach and cutback operating conditions. Computations for the two most relevant frequencies were made. Results show that generally significant reductions up to 11 dB can be achieved with technically acceptable control parameter values at the optimum.

Nomenclature

A	= vane vibration amplitude (radians), Eq.(2)
B	= number of vanes
c	= vane chord
D	= angular position of zeroth vane
h	= hub/tip ratio
i	= imaginary unit
k	= circumferential harmonic incident wakes
M	= axial flow Mach number
$\boldsymbol{n}$	= unit normal on vane surface, Eq.(1)
t	= time
$U_{m\mu}$	= radial eigenfunction , Eq.(7)
$\boldsymbol{v}$	= velocity
x	= axial coordinate
x_L	= axial position of leading edge
x_M	= axial mid chord position, Eq.(5)
x_P	= axial position of pitch axis, Eq.(2)
x_T	= axial position of trailing edge
β	= $\sqrt{1-M^2}$
δ_{ik}	= Kronecker delta symbol, Eq.(6)
ζ	= transformed radial coordinate, Eq.(4)
θ	= circumferential coordinate, Eq.(7)
ξ	= axial source coordinate, Eq.(7)
ρ	= radial source coordinate, Eq.(7)
φ	= transformed chordwise coordinate, Eq.(5)
ω	= Helmholtz number (nondim. freq.), Eq.(2)

*Senior Research Engineer, Aeroacoustics Department P.O.Box 153, E-mail: schulten@nlr.nl, Senior Member AIAA.

Introduction

Fan noise has been a major component in subsonic transport aircraft noise for many years. Continual improvement of acoustic engine design has brought a substantial noise reduction. However, further suppression is getting more and more difficult and it is not to be expected that fan noise can be completely eliminated by a more sophisticated rotor-stator layout and duct lining alone. Therefore, active noise control (ANC) of fan noise has received considerable attention over the past ten years. A comprehensive review of the current state of the art in ANC has been given by Peake and Crighton[1]. With a few exceptions most of the work in the field of turbofan ANC has been concentrated on (piezo-electric) surface actuators mounted either in the vanes or in the duct walls. A technical discussion of vane mounted surface actuators has been given by Simonich[2]. The use of an actuated trailing edge flap on a single airfoil was studied theoretically by Kerschen[3] and experimentally by Simonich et al.[4]. Reductions up to 10 dB over portions of the acoustic spectrum were reported.

In the present paper the effect of a controlled oscillatory motion of vanes pitching about a spanwise axis is considered. The goal is first to present a method to optimize the control parameter settings and secondly to apply this tool to assess the noise reduction potential of vanes vibrating in pitch [Fig.1]. Of course, the mechanical implications of such a system are enormous. On the other hand, the potential of sound reduction could be large as well and the system has to be active during takeoff and landing only. To find the maximum theoretical sound reduction some control parameters will have to be varied systematically. The control parameters, i.e. the degrees of freedom, that will be used in this study are the amplitude, phase and axis location of the pitching motion. The function to be minimized will be either the upstream or the downstream acoustic intensity or a combination of both.

Figure 1 In pitch vibrating vane

Theoretical method

In the present study a lifting surface modeling of the problem will be used. This is an approximation in which the interaction problem of wakes and vanes is linearized about an inviscid, uniform mean flow. Since the vanes are, to leading order, parallel to the uniform flow, the boundary condition to be satisfied at the vane surfaces reads:

$$\boldsymbol{n} \bullet \boldsymbol{v}_{induced} = \boldsymbol{n} \bullet (\boldsymbol{v}_{vane} - \boldsymbol{v}_{incident}) \qquad (1)$$

Since $\boldsymbol{v}_{induced}$ is an integral containing the unknown vane pressure jump distribution, Eq.(1) is an integral equation. The equation is the same as in the common rotor–stator interaction problem except for the appearance of the vane velocity in the right hand side. This means that an existing theory[5] can be used with only minor changes. It also implies that the time consuming computation of the left-hand side has to be made only once because alterations of the control parameters only affect the right hand side. This property is extremely advantageous in an optimization compared to a field (CFD/CAA) method requiring a completely new calculation for any change of the control parameters.

If the instantaneous angle of incidence of a vibrating vane is denoted by $A\ \exp(i\omega t)$ the normal vane velocity resulting from pitching about an axis at x_P is to leading order given by

$$\boldsymbol{n} \bullet \boldsymbol{v}_{vane} = i\omega A(x - x_P)\exp(i\omega t) \qquad (2)$$

where x_P is the axial position of the pitch axis. Clearly, to achieve any sound reduction at all, the angular frequency ω must be equal to that of the incident rotor wake harmonic considered. The numerical solution of Eq.(1) involves a chordwise and spanwise Galerkin projection as follows

$$\int_0^{\pi} \cos j\zeta \int_0^{\pi} \sin(\ell+1)\varphi \sin\varphi \ \ \boldsymbol{n} \bullet \boldsymbol{v}_{induced}\, \mathrm{d}\varphi\, \mathrm{d}\zeta = \int_0^{\pi} \cos j\zeta \int_0^{\pi} \sin(\ell+1)\varphi \sin\varphi \ \ \boldsymbol{n} \bullet (\boldsymbol{v}_{vane} - \boldsymbol{v}_{incident})\, \mathrm{d}\varphi\, \mathrm{d}\zeta \qquad (3)$$

for $\ell = 0, \ell_{\max}, \ j = 0, j_{\max}$

where

$$r = \frac{1+h}{2} + \frac{1-h}{2}\cos\zeta\ , \qquad (4)$$

and

$$x = x_M + \frac{c}{2}\cos\varphi\ , \ \text{with}\ x_M = (x_L + x_T)/2 \qquad (5)$$

In previous work[5] the same Galerkin projection was used for the spanwise and chordwise directions. It has been found, however, that for ducted fans the presently used first kind Chebyshev ($\cos j\zeta$) projection in the spanwise direction yields better results. For instance, the resulting pressure jump distribution more accurately satisfies the end wall boundary conditions at hub and tip.

It is interesting to note that the present vane motion yields only two nonzero Galerkin projections. Substitution of Eq.(2) in the right hand side of Eq.(3) yields

$$\int_0^{\pi} \cos j\zeta \int_0^{\pi} \sin(\ell+1)\varphi \sin\varphi \ \ \boldsymbol{n} \bullet \boldsymbol{v}_{vane}\, \mathrm{d}\varphi\, \mathrm{d}\zeta = i\omega A \exp(i\omega t)\frac{\pi^2}{2}\delta_{j0}\left[(x_M - x_P)\delta_{\ell 0} + \frac{c}{4}\delta_{\ell 1}\right] \qquad (6)$$

Due to the absence of a radial dependence only the $j = 0$ projection can be nonzero. Further, the pitching motion about an axis at x_p can always be represented by a rotation about mid chord and a plunging motion as shown in the right hand side of Eq.(6) by the Kronecker delta symbols.

Numerical examples

Geometry and operating conditions

To study the effects of vibrating stator vanes numerically, the same example of a generic fan stage as used in a recent study[6] was chosen. Data and (approach) operating conditions are listed in Table 1, in which all dimensions are scaled on the duct radius. As usual in current fans, the 1st harmonic of the blade passing tones is cut-off. In the 2nd harmonic an $m = 1$ circumferential mode is generated with 6 radial modes cut-on.

Table 2 shows a part of the absolute values of the right hand side elements of Eq.(3) for fixed vanes, scaled on the largest element. As found above [Eq.(6)], vane vibration can affect only the upper left elements (0,0) and (1,0), which are rather small compared to the largest element (4,0). Furthermore, controlled vibration cannot cancel both the (0,0) and

Table 1 Fan data

Number of rotor blades	23
Number of stator vanes	47
Hub/tip ratio h	0.50
Vane chord length	0.12
Axial Mach number	0.32
Rotor tangential tip Mach number	0.75
Axial extent rotor chord	0.15
Rotor blade drag coefficient	0.05
Nondim. 2nd harmonic frequency	34.50
Rotor-stator gap	0.2

Table 2 Scaled absolute values of right hand side elements for fixed vanes

J =	0	1	2	3	4
L = 0	0.168	0.025	0.006	0.007	0.004
L = 1	0.344	0.037	0.030	0.007	0.006
L = 2	0.320	0.033	0.013	0.008	0.004
L = 3	0.754	0.083	0.031	0.005	0.002
L = 4	1.000	0.080	0.054	0.007	0.005
L = 5	0.878	0.046	0.054	0.002	0.005
L = 6	0.594	0.017	0.032	0.006	0.002
L = 7	0.329	0.011	0.013	0.004	0.003
L = 8	0.154	0.009	0.003	0.006	0.005
L = 9	0.061	0.007	0.004	0.006	0.005
L =10	0.017	0.004	0.004	0.003	0.002

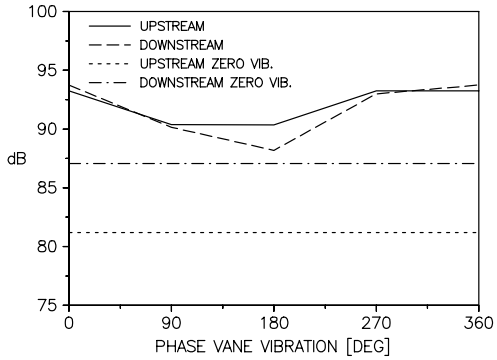

Figure 2 Phase variation, amplitude 0.1 deg., pitch axis 50%.

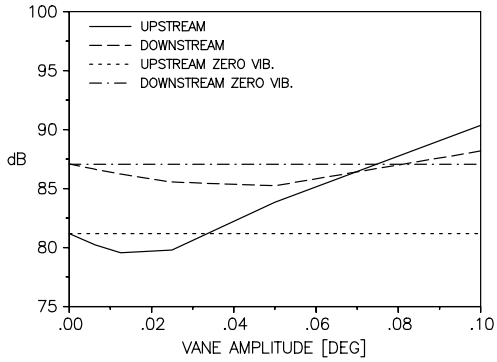

Figure 3 Amplitude variation, phase angle 180 deg., pitch axis 50%.

(1,0) motions simultaneously, because they both have the same phase, set by the amplitude *A*, see Eq.(6).

An unskilled optimization

In order to get a first idea of how the sound level in the 2nd harmonic depends on the control parameters, we will carry out a full iteration cycle of the process by hand. From the magnitude of the right hand side of the integral equation a first guess of the required amplitude *A* is made. In the present example one tenth of a degree is taken. The starting location of the pitch axis is chosen at 50 percent of the chord. Fig.2 shows the computed upstream and downstream acoustic intensity as a function of the phase of *A*. Without any vibration the levels are 86.6 dB downstream and 81.2 dB upstream. It appears that for this amplitude there is no phase that improves upon the zero vibration level. However, we still can observe that a phase angle of about 180 degrees gives the lowest acoustic intensity downstream.

Next, the amplitude is varied for constant phase and axis location. The result in Fig.3 shows that different optimum values are found for the upstream and downstream intensity. The upstream intensity is the lower one and has an optimum amplitude of about 0.02 degree, whereas the downstream intensity requires an optimum amplitude of 0.05 degree. To

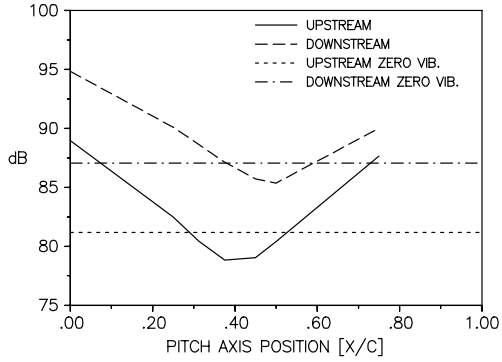

Figure 4 Pitch axis position variation, amplitude 0.03 deg., phase angle 180 deg

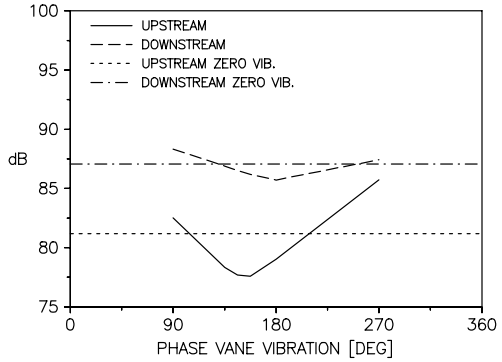

Figure 5 Phase variation, 2nd iteration cycle, amplitude 0.03, pitch axis at 45%

continue we adopt an amplitude of 0.03 degree for the variation of the location of the pitch axis.

As Fig.4 shows, there is a quite remarkable sensitivity on the axis location. A best location of about 40 % is found for the upstream location and of 50 % for the downstream location. Taking the average of 45 % as a compromise, we start the second full iteration cycle with the phase variation. As shown in Fig.5 we now obtain a quite marked optimum for the upstream intensity at a phase angle of about 150 degrees. So after 4/3 iteration cycle the reduction with respect to fixed vanes is already 4.5 dB. The downstream optimum is closer to 180 degrees and has a total reduction of 1.5 dB only. Although we could continue this way to find an optimum configuration, it is preferable to use a more intelligent routine optimization technique.

Optimization technique

To optimize amplitude, phase and pitching axis location for a given case, the *Downhill Simplex Method in Multidimensions* of Nelder and Mead, described in Ref.7, Ch.10, was implemented. This method requires only function evaluations, not derivatives. Further, the whole cycle of lifting surface programs (from vibration velocity to acoustic intensity calculation) is comprised in a single function. Its value is either the upstream-radiated acoustic intensity or the

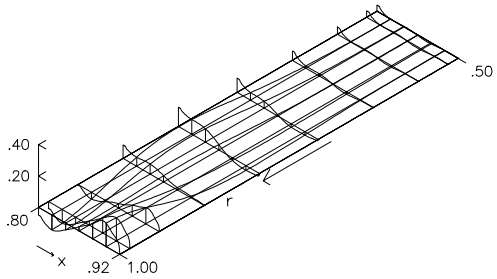

Figure 6 Real part Δ*Cp*, 2nd harmonic, fixed vane.

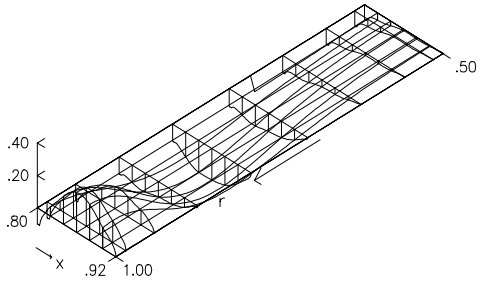

Figure 7 Imaginary part Δ*Cp*, 2nd harmonic, fixed vane

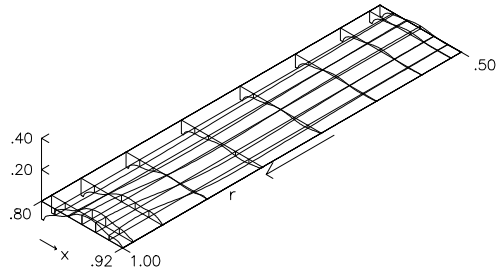

Figure 8 Real part Δ*Cp*, 2nd harmonic, vibrating vane

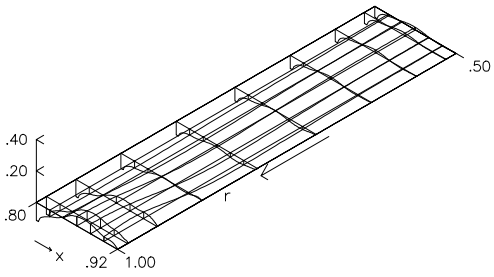

Figure 9 Imaginary part Δ*Cp*, 2nd harmonic, vibrating vane

downstream intensity or any (linear or nonlinear) combination of both. The viscous rotor wake calculation is computed outside the iteration loop, as is the time consuming influence matrix. A full optimization typically takes half an hour on a 300 MHz Pentium II.

Optimization of 2nd harmonic

In Table 3 the results of the above minimization method are presented. When applied to the upstream noise (first row), a reduction of 8.5 dB can be attained. At the same time the downstream noise is still reduced by 5.7 dB. Note that this is quite an improvement on our iteration cycle by hand above. The optimum amplitude is only 0.0134 degree, while the pitch axis is remarkably close to the trailing edge.

As shown in the second row of Table 3, the downstream noise can be even better reduced with a surprising 11.1 dB. However, to achieve this the amplitude has to be more than twice as large as for minimum upstream noise and also the other parameters are different. As a result the upstream reduction is only 3.0 dB.

In practice it will be of interest to minimize some combination of upstream and downstream noise. As an example the results for the sum (in dB) of the upstream and downstream acoustic intensity are given in the last row of Table 3. Apparently, for this case both the upstream reduction of 6.6 dB and the downstream reduction of 9.2 are almost 2dB lower than the maximum achievable in each direction independently.

These are remarkably substantial reductions considering the limited degrees of freedom of rigid vanes vibrating in pitch.

Pressure jump distribution

To obtain some understanding of the mechanism underlying the sound reduction discussed above, it is useful to consider the vane pressure jump distributions. In figures 6 and 7 the 2nd harmonic of the unsteady pressure jump distribution for a fixed vane is shown. The results of vane vibration optimized for minimum upstream noise are given in figures 8 and 9. Especially the reduction of the imaginary part of the vane pressure response is remarkable, cf. Fig.7 with Fig.9. For this case, low order, simple motions appear to be very effective on this point.

Of course, a small pressure response is not enough for a low noise emission but it certainly helps in general. In the end the coupling of the pressure jump distribution with the cut-on acoustic duct modes determines the resulting noise emission. The expression

Table 3 Minimization of 2nd harmonic interaction noise

Minimization	Upstream Reduction (dB)	Downstream Reduction (dB)	Amplitude (deg.)	Phase (deg)	Pitch axis (% chord)
Upstream	8.5	5.7	0.0141	78.0	79.8
Downstream	3.0	11.1	0.0311	108.7	65.7
Up+Down	6.6	9.2	0.0210	96.8	71.3

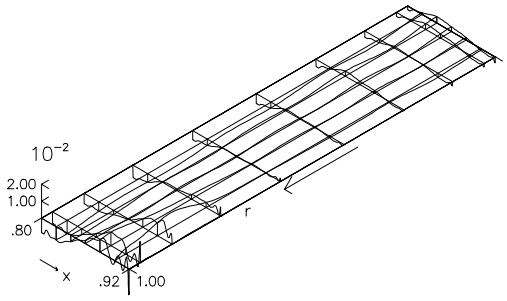

Figure 10 Real part Δ*Cp*, 3rd harmonic, fixed vane.

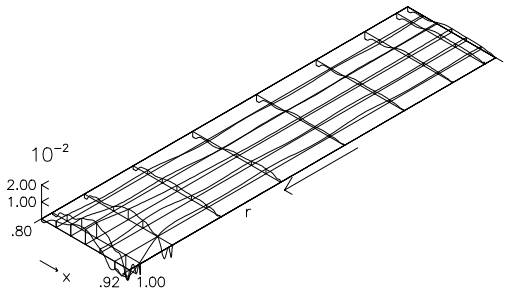

Figure 11 Imaginary part Δ*Cp*, 3rd harmonic, fixed vane.

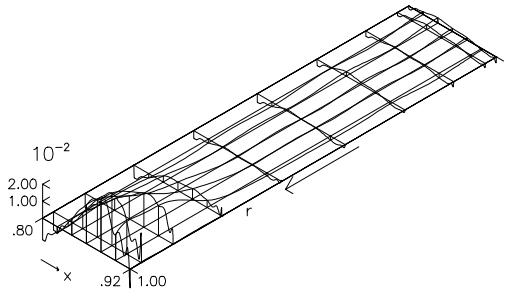

Figure 12 Real part Δ*Cp*, 3rd harmonic, vibrating vane.

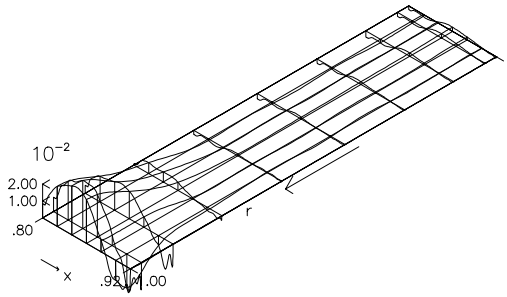

Figure 13 Imaginary part Δ*Cp*, 3rd harmonic, vibrating vane.

for the pressure generated by the unsteady pressure jump over the vanes is given by[5,6]:

$$\tilde{p}(x,r,\theta,t)=\frac{-B}{2\pi}\exp(i\omega t)\sum_{n=-\infty}^{\infty} m\ \exp\left[im\left(\theta-D\right)\right] \times\sum_{\mu=1}^{\infty}\frac{U_{m\mu}(r)}{2\beta_{m\mu}(\omega)}\int_{h}^{1}\frac{U_{m\mu}(\rho)}{\rho} \tag{7}$$

$$\times\int_{x_L}^{x_T}\exp\left[i\frac{(x-\xi)}{\beta^2}\left\{M\omega-\mathrm{sgn}(x-\xi)\beta_{m\mu}(\omega)\right\}\right] \times\Delta p(\xi,\rho)\,\mathrm{d}\xi\mathrm{d}\rho$$

$$\text{with}\qquad m=k-nB \tag{8}$$

and where the complex function $\beta_{m\mu}$ can be found in Ref.5 or 6.

Expression (7) is an expansion in duct modes in which the modal amplitudes are given by a double integral over the reference vane. Of course, this integral will be small if Δp is small. The other possibility to obtain a small modal amplitude is a poor coupling, i.e. a mismatch, between Δp and the modal radial and axial shapes. Note that the double integral also implies double possibilities for modal mismatch. Clearly, for a given Δp a poor coupling can only be achieved for a rather limited number of modes. Consequently, if the number of cut-on modes, which carry the propagating sound, is really low, modal mismatch has great sound reduction potential.

Third harmonic optimization

It is interesting to see if for the third harmonic of the interaction noise a similar reduction can be obtained as for the second harmonic. In terms of annoyance the third harmonic is still very relevant for most turbofans. For instance with a diameter of two meters, the third harmonic of the present fan would be 2800 Hz.

In the third harmonic, interaction sound is generated in two circumferential mode numbers: m = -22 with 8 radial modes cut-on and m = 25 with 7 radial modes cut-on. As discussed above, this relatively large number is unfavorable for active sound reduction. For fixed vanes the total upstream noise level is 78.8 dB and the downstream level 81.5 dB.

As shown in Table 4, relatively small noise reduc-

Table 4 Minimization of 3rd harmonic interaction noise

Minimization	Upstream Reduction (dB)	Downstream Reduction (dB)	Amplitude (deg.)	Phase (deg)	Pitch axis (% chord)
Upstream	3.1	-4.0	0.000909	-123.7	44.8
Downstream	-4.4	5.6	0.00107	18.3	42.1
Up+Down	1.9	-0.6	0.000255	-70.9	14.3

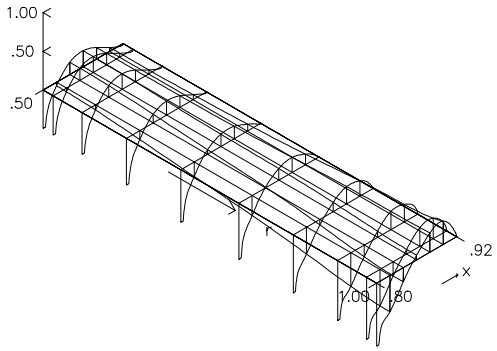

Figure 14 Real part Δ*Cp*, 1st harmonic high speed case, fixed vane

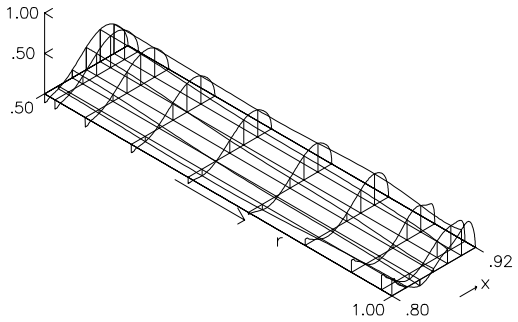

Figure 15 Imaginary part Δ*Cp*, 1st harmonic high speed case, fixed vane

tions are obtainable with controlled vibration. The best result is 5.6 dB reduction for downstream optimization. However, for this condition there is an increase of 4.4 dB at the upstream side. As similar situation is found for upstream optimization. The last row of Table 4 shows that optimization for the combined levels yields an optimum of only 1.3 dB: an upstream reduction of 1.9 dB and a downstream increase of 0.6 dB.

The pressure jump distribution for fixed vanes is given in Figs. 10 and 11. Roughly speaking, the vane pressure response is only a tenth of the second harmonic response. The third harmonic of the incident wakes also yields a rather corrugated pressure response.

The resulting pressure response for minimum downstream noise is presented in Figs. 12 and 13. Despite the substantial increase of the response in the tip region, this is the pressure jump distribution that yields a downstream reduction of 5.6 dB. As already mentioned above, the coupling with the upstream propagating modes is less favorable and leads to an increase of 4.4 dB.

A higher speed case

To avoid jumping into conclusions based on just one rotor speed, it was considered worthwhile to study also a case with a higher rotor speed. Therefore, the same fan was taken as given in Table 1, but now with a tangential tip Mach number of unity. The axial

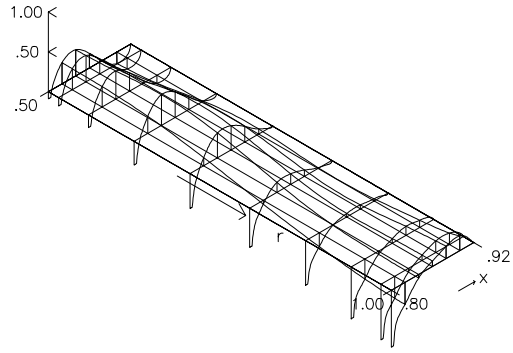

Figure 16 Real part Δ*Cp*, 1st harmonic high speed case, vibrating vane

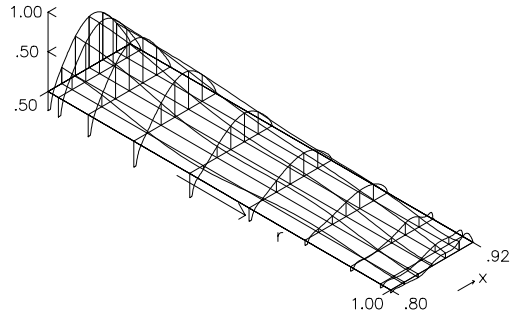

Figure 17 Imaginary part Δ*Cp*, 1st harmonic high speed case, vibrating vane.

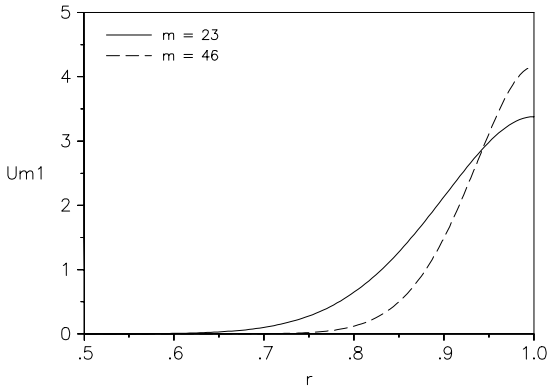

Figure 18 First radial order eigenfunctions for high speed case

Mach number was increased proportionally to M = 0.4267. These conditions are typical for the power cutback after takeoff. An interesting aspect of this higher rotor speed is that the first harmonic of the blade passing frequency is just cut-on.

1st harmonic optimization In the first harmonic one radial mode with $m = 23$ is cut-on. This circumferential mode number is the same as the number of rotor blades. While in an actual fan stage the so-called rotor-alone noise will cut on at exactly the same speed, we will restrict ourselves here to the sound

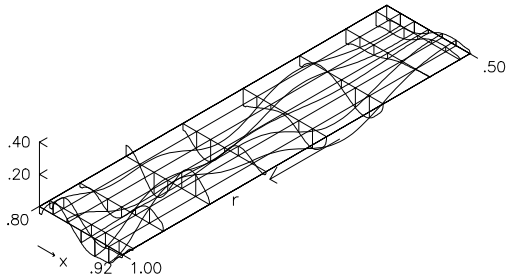

Figure 19 Real part Δ*Cp*, 2nd harmonic high speed case, fixed vane.

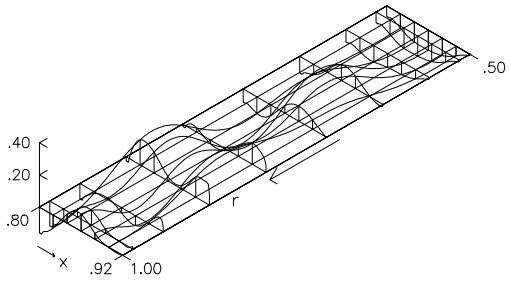

Figure 20 Imaginary part Δ*Cp*, 2nd harmonic high speed case, fixed vane.

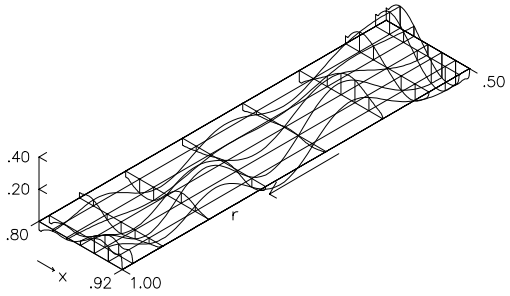

Figure 21 Real part Δ*Cp*, 2nd harmonic high speed case, vibrating vane.

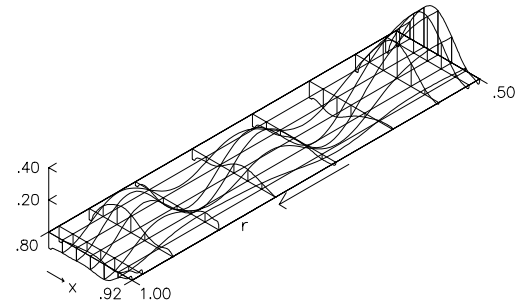

Figure 22 Imaginary part Δ*Cp*, 2nd harmonic high speed case, vibrating vane.

generated by interaction of rotor wakes with the stator.

With an upstream level of 115.9 dB and 119.8 dB downstream the noise level is considerably higher than in the previous cases. This can be explained by the magnitude of the 1st wake harmonic compared to higher wake harmonics[6].

As shown in the first row of Table 5, the upstream noise can be completely suppressed by controlled vane vibration. The achieved reduction of 129.5 dB really implies complete silence by any human standard. Surprisingly, only 1.1 dB reduction is obtained for this condition at the downstream side of the stator. Note that with 0.682 degrees the amplitude of the vibration is also much larger than in the previous cases.

A similarly outstanding result can be obtained at the downstream side where a maximum reduction of 114.6 dB is achieved. Unfortunately, the upstream noise increases by 5.4 dB for this condition. Note the peculiar position of the pitch axis at almost 1 chord length upstream of the leading edge. This means that the vibration is dominated by the plunging (0,0) component As the third row of Table 5 shows, the combined optimization criterion gives the same result as optimization for upstream noise alone.

To a certain extent the radial mode shape, shown in Fig.18 can explain the amazing sound suppression found for this case. It appears that only beyond a radius of 0.7 the pressure jump is of importance, which makes optimization easier. Indeed, a decrease of the pressure response in the tip region can be observed in Figs.14-17. However, this is by far not enough to explain the superb suppression performance found. Apparently, the chordwise pressure can also be modified by vibration such that a virtually perfect mismatch with the modal axial dependence is obtained [Eq. (7)]. It is surprising that this can be achieved for both the upstream and downstream sides, although not simultaneously.

2nd harmonic To have a more direct comparison with the lower speed case we will investigate now the second harmonic of the high speed case. The nondimensional frequency of the second harmonic

Table 5 Minimization of 1st harmonic, high speed case interaction noise

Minimization	Upstream Reduction (dB)	Downstream Reduction (dB)	Amplitude (deg.)	Phase (deg)	Pitch axis (% chord)
Upstream	129.5	1.1	0.682	102.0	43.9
Downstream	-5.4	114.6	0.248	-153.5	-99.8
Up+Down	129.5	1.1	0.628	102.0	43.9

equals 46, which is twice the number of rotor blades. Like in the lower speed case, interaction sound is generated in circumferential mode number: m = 1, now with 9 radial modes cut-on. However, there is also an m = -46 with 1 radial mode cut-on. The latter one is comparable with the mode m = 23 in the 1st harmonic.

For fixed vanes an upstream level of 96.0 dB is found and downstream a level of 96.9, both of which are considerably higher than in the lower speed case, but at the same time some 20 dB lower than in the 1st harmonic above. The m = -46 mode is almost entirely responsible for this level. As Table 6 shows, a quite acceptable reduction of 11.4 dB is possible for the upstream propagating noise. A maximum reduction of 8.4 dB in the downstream direction also is a good performance.

The pressure jump distribution over the fixed vanes is shown in Figs. 19 and 20. Its character is different from the lower speed case as it shows more spanwise waviness. In Figs. 21 and 22 the pressure response for vibrating vanes optimized for minimum upstream noise is shown. Surprisingly, the pressure jump at the hub is considerably larger than for the fixed vanes. Apparently, the optimization procedure takes advantage of the shape of the eigenfunction for m = -46 which is virtually zero up to a radius of 0.8 [Fig.18]. It can concentrate on the outer part of the vanes and does not have to bother about the consequences for the inner part. It is another example of the fact that a poor coupling between pressure jump distribution and modes is more important than just a low pressure response itself.

Discussion

As shown in the previous section substantial reductions of more than 10 dB are possible by active vane control. For special cases sound emission may even be annihilated completely by controlled vane vibration. The obvious question arises if vane vibration methods can be combined with other noise reduction measures such as swept vanes to promote a further noise reduction. Unfortunately this seems to be impossible for vane sweep since the sound reduction by pitching vane vibration can only work if the rotor wakes hit the vane leading edge in phase all along the span. Vane sweep introduces a spanwise phasing which excludes the benefits of vane vibration. In fact a rather fancy phased vane pitch control in the spanwise direction would be required to recover these benefits.

Furthermore it is to be noted that in real turbomachines there is usually a considerable swirl induced spanwise phasing of the wake impingement. This will reduce the noise reduction potential of active vanes for the same reason as discussed above in the context of vane sweep. Only in case of a "solid block" swirl (constant angular velocity for all radii) no radial phasing is induced and may the full potential of vibrating vanes be conserved. In general the results presented in this paper rather give an upper limit of what could be achieved by active vanes under ideal conditions than numbers one can apply straightaway to the Outlet Guide Vanes (OGV) of an arbitrary turbomachine. It is noted that the first Engine Section Stator (ESS) may be a more suitable candidate for active vibration, also because of probable constraints in the application of vane sweep and lean. Due to the smaller height of the core engine intake duct, the swirl induced spanwise phasing will be considerably smaller, which will enhance the effectiveness of active vane vibration. Also, the ESS optimization can be limited to the forward noise only.

Concluding remarks

It has been demonstrated that, at least in theory, noise control with vanes vibrating in pitch is feasible and sometimes very effective.

A lifting surface method for the computation of rotor-stator interaction noise was successfully extended with the effect of controlled vane vibration about a pitching axis.

Most numerical methods would be prohibitively expensive for optimization but for a given incident rotor wake system a lifting surface method only needs minimal computation time for parameter variation.

The *Downhill Simplex Method in Multidimensions* was implemented as optimization technique. It performed quite well for the present problem and requires typically 50-100 steps for an accuracy of 0.1 dB.

Considerable noise reduction through active vane control can be achieved. More specifically, a maximum reduction in the order of 10 dB, both forward and aft, of noise was found for a number of typical cases.

The major sound reduction mechanism in controlled vane vibration appears to be the promotion of a poor coupling between pressure jump and cut-on modes. The lower the number of cut-on modes, the better this modal mismatch principle works. In some special cases complete sound suppression was accomplished.

Table 6 Minimization of 2nd harmonic, high speed case interaction noise

Minimization	Upstream Reduction (dB)	Downstream Reduction (dB)	Amplitude (deg.)	Phase (deg)	Pitch axis (% chord)
Upstream	11.4	6.8	0.0501	102.8	61.4
Downstream	5.9	8.4	0.0328	108.9	76.0
Up+Down	11.2	7.3	0.0493	103.7	63.3

Acknowledgement

The development of the method was partially sponsored by the BriteEuram RESOUND project of the European Union.

References

[1]Peake, N., Crighton, D.G., "Active Control of Sound", *Annual Rev. Fluid Mech*., 2000, Vol.32, pp.137-164.

[2]Simonich, J.C., "A Review of Actuators for Active Noise Control in Gas Turbines", Proc. 1st Joint CEAS/AIAA Aeroacoustics Conference, Munich, June 1995

[3]Kerschen, E.J., "Active Aerodynamic Control of Wake Airfoil Interaction Noise - Theory", Proc. DGLR/AIAA 14th Aeroacoustics Conf., Aachen, May 1992.

[4]Simonich, J.C., Lavrich, P.L., Sofrin, T.G., Topol, D.A., "Active Aerodynamic Control of Wake Airfoil Interaction Noise - Experiment", Proc. DGLR/AIAA 14th Aeroacoustics Conf., Aachen, May 1992.

[5]Schulten, J.B.H.M., "Vane Sweep Effects on Rotor/Stator Interaction Noise," *AIAA Journal*, Vol.35, No.6, June 1997, pp.945-951.

[6]Schulten, J.B.H.M., "Unsteady Leading-Edge Suction Effects on Rotor-Stator Interaction Noise," *AIAA Journal*, Vol.38, No.9, September 2000, pp.1579-1585.

[7]Press, W.H., Flannery, B.P., Teukolsky, S.A., Vetterling, W.T., *Numerical Recipes*, Cambridge University Press, 1989